



Research Article

Thermal analysis of PCM-based hybrid micro-channel heat sinks: A numerical study

Korasikha Naga RAMESH¹, Thopudurthi Karthikeya SHARMA^{1,*}

¹Department of Mechanical Engineering, NIT Andhra Pradesh, 534101, India

ARTICLE INFO

Article history

Received: 25 April 2022

Accepted: 05 September 2022

Keywords:

Thermal Management;
Electronic Cooling; Hybrid
Micro-Channel Heat Sink; Phase
Change Material (PCM); Liquid
Fraction; Thermal Performance

ABSTRACT

Heat sinks play a vital part in the heat dissipation in electronic devices and energy systems. Heat generation in the present-time electronic equipment is very high because of the high power density and the miniaturization of the components. An efficient and high-capacity thermal management system is needed for the efficient performance of the latest electronic equipment. Micro-channel heat sinks (MCHS) are an effective solution for the cooling of electronic devices in view of large heat dissipation and compactness. The performance improvement in the MCHS is the prime focus of most of the researchers. In the present work, the improvement of heat transfer in MCHS with the introduction of phase change material (PCM) was investigated numerically with the help of ANSYS-FLUENT. The finding of the computational model applied for the present numerical work was compared with existing literature and noticed a good agreement with both experimental and simulation studies. The performance of three different PCM-based hybrid MCHS models was studied and compared with the model of MCHS without PCM using the parameters, thermal resistance, temperature uniformity, liquid fraction, and Nusselt number. A good augmentation in the performance of PCM-based MCHS with a maximum 7.3% decrement in thermal resistance and 15.26% increase in temperature uniformity was observed. 3-dimensional variation of the liquid fraction with Reynolds number and heat flux is also presented.

Cite this article as: Ramesh KN, Sharma TK. Thermal analysis of PCM-based hybrid micro-channel heat sinks: A numerical study. J Ther Eng 2023;9(4):1015–1025.

INTRODUCTION

The miniaturization and multi-functionality of modern electronic equipment lead to overheating of electronic components, which dramatically increases their operating temperature. High working temperatures reduce the electronic components' efficiency and life [1,2]. Over 55% of failures in electronic components are because of high working

temperatures[3]. Therefore an efficient thermal management system is needed to avoid failures due to overheating of electronic components. Researchers are developing innovative solutions for heating issues in electronics. The micro-channel heat sink (MCHS) is an efficient heat dissipating device for electronics and it was first introduced by DB Tukermann [4] in 1981. Their work increased the research focus on micro-channel based heat sinks for

*Corresponding author.

*E-mail address: knramesh.sclr@nitandhra.ac.in, tks@nitandhra.ac.in

This paper was recommended for publication in revised form by Editor in Chief Ahmet Selim Dalkilic



electronic cooling applications [5]. Researchers implemented different methods like modifying the geometry, using different working fluids and implementing different flow configurations etc., to enhance the thermal performance of the Micro-channel heat sink (MCHS) [6,7]. Numerous research works on the influence of geometry [8–10] and channel shape [11,12] on MCHS performance have been noticed in the literature [13]. Amirah M. Sahar et al. [14] examined the influence of aspect ratio (AR) and hydraulic diameter on heat transfer in a rectangular MCHS. They noticed a little decrease of friction factor with increasing the AR up to 2 then starts increasing with increasing the AR. The increase of Nusselt number with hydraulic diameter was also observed for thermally and hydro-dynamically developed flow.

Yan Ji et al. [15] examined the flow of compressible gas in an MC with Mach number at the inlet was ranged from 0.0055 to 0.202. They found the noticeable influence of surface roughness on the gas flow at a smaller Knudsen number (Kn). The increase in Poiseuille's number was noticed with rising the roughness height and decreasing the space among the roughness elements. Soheil S et al. [16] conducted a numerical study on MCHS with channels in transverse direction. They reported that the Nu and pressure loss increases with reducing the height of the channel and increasing the transverse channels count. Guilian Wang et al. [17] examined the enhancement of heat transfer in MCHS with vertical ribs, spanwise ribs and bidirectional ribs. It was observed that for bidirectional ribbed MCHS, the Nu is 1.2–1.42 and 1.4–2 times to the span-wise ribbed and vertical ribbed MCHS respectively. The authors also mentioned both Vertical and span-wise ribs can disturb the thermal boundary layer and generate the recirculation of the flow. Yanjun Zhang et al. [18] conducted simulation analysis on MCHS with a slot-jet module to scrutinize the influence of the channel shape on its thermal performance. In this study, the lowest module temperature was found in the Trapezoid channel. They also reported that the rectangular channel is not helpful for jet impingement to develop the vortices.

A numerical investigation done by Navin Raja Kuppusamy et al. [19,20] on MCHS with Nano-fluid based triangular shaped and trapezoidal shaped grooves achieved an improvement in its performance. They also noticed the superior performance of MCHS with trapezoidal grooves compared to rectangular. Z Yari Ghale et al. [21] conducted a simulation study on Ribbed MCHS with the nano-fluid flow and revealed that the 2-phase model is exact compared to 1-phase model. The mean discrepancy of the 2-phase mixture model and 1-phase model from experimental findings are 11.39% and 32.6% respectively. Eyuphan Manay et al. [22] conducted an experimental analysis on the effect of volume fraction of TiO_2 -water nano-fluid and channel height on both friction and thermal entropy generation in MCHS. The authors witnessed an increase in the friction and thermal entropy from 3.3% to 21.6% and 1.8 to 32.4%

respectively with increasing the volume fraction in the studied range. They also reported that the thermal entropy increases and frictional entropy decrease with increasing the channel height.

In the Eulerian-Lagrangian 2-phase model study conducted on a wavy micro-channel, J Rostami et al. [23] investigated the conjugate heat transfer with Al_2O_3 -water nano-fluid. J Rostami et al. observed an increase in pressure loss and heat transfer rate in wavy channelled heat sink than straight channelled due to the recirculation zones and secondary flows. Muhammed Saeed et al. [24] performed the numerical analysis on the hydrothermal behaviour of an MCHS using supercritical Carbon dioxide ($s\text{CO}_2$) as a working fluid. It was found that, with using the supercritical carbon dioxide the performance of MCHS is augmented by 2.2 times compared to the water. Pressure drop was also noticed to be reduced by up to 7 times compared to water.

From the literature mentioned above it is noted that the attention of most researchers is to enhance the heat transfer in MCHSs by augmenting the effective heat transfer area and improving the working fluid characteristics. Along with these methods Phase changing materials (PCM) are also used in MCHS. Phase change materials (PCM) got a huge focus of researchers working on thermal management applications since their advantage of high latent heat capacity [25–27]. Researchers modelled heat sinks with Phase changing materials (PCM) and showed the improvement in the heat transfer performance. Xunjia Deng et al. [28] explored the heat transfer characteristics of micro-encapsulated PCM (MEPCM) slurry flow in MCHS by introducing the fin and the porous media. Over estimation of heat sink performance was noticed in case of the method using fin due to the consideration of dimension less temperature as a constant in the perpendicular direction to the flow. Up to 25% decrement in thermal resistance of MCHS was observed in thermal analysis done by C.J. Ho et al. [29] on divergent micro-channel. For this work water-based MEPCM suspensions was used as a working fluid. W Yan et al. [30] investigated the MCHS with PCM filled in the ceiling and water- Al_2O_3 Nano-fluid was used as working fluid. They found the 10.88% decrement in heat sink thermal resistance at Nano particle concentration of 10% and Re 500.

From the literature, it was realized that the focus of most of the research works of MCHSs is on the enhancement of their thermal performance by modifying the channel structure, adding the extended surfaces, changing the flow pattern and using better working fluid etc. The maximum heat removed by these heat sinks is constant at a particular flow rate. To manage fluctuations in the heat generated by an electronic device, heat sinks have to run with full capacity and that need more electric power. PCM-based passive heat sinks can manage this issue to some extent but they are effective during the phase changing process only. The novel PCM-based hybrid MCHS model developed in this work has the advantages of both energy storage and convective

heat transfer, and has the ability to manage the variable heat generation. In the literature, there is no prominent work on PCM-based hybrid MCHS was noticed. There is high scope for advancement of Hybrid MCHS for electronic cooling.

In the present numerical study three novel designs of hybrid MCHS are developed by incorporating the PCM. The Numerical modelling was done using ANSYS-FLUENT and results were validated with existing numerical and the experimental results. The performance of these hybrid MCHS models is compared with model without PCM. A significant improvement in the thermal performance is noticed in hybrid MCHS.

PHYSICAL MODEL

The 3-Dimensional view of computational domain used for present simulation analysis is shown in Figure 1. The heat transferred to the heat sink by the heat source was dissipated by the working fluid flowing in the micro-channels. The PCM was filled in the provision provided below the channels. This heat sink was mainly designed to withstand the fluctuations in the heat generated by the source and it is well suitable for electronic cooling because of the transient nature of heat generated by the electronic components.

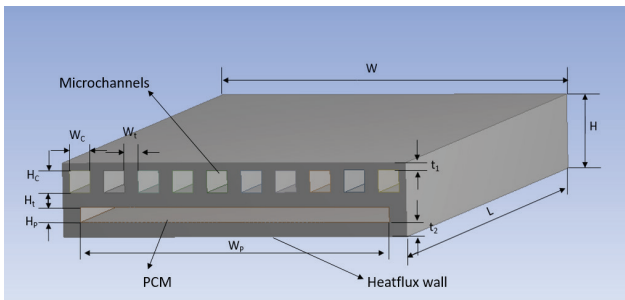


Figure 1. The schematic image of the MCHS.

W_C , W_P and W are the width and H_C , H_P and H are the height of the micro-channel, PCM layer, and heat sink respectively and L is the MCHS length. W_t is the web thickness between micro-channels and t_1 and t_2 are MCHS upper and lower rib thickness. These dimensions are provided in Table 1.

Table 1. Considered dimensions of heat sinks

Heat sink dimensions			
W	5 mm	H_p	0.2 mm
W_C	0.3 mm	L	10 mm
W_P	4.5 mm	W_t	0.2 mm
H	1 mm	t_2	0.2 mm
H_C	0.3 mm	t_1	0.1 mm

Copper and water are considered as the MCHS material and working fluid for the present simulation analysis. Paraffin is the phase change material (PCM) introduced in the heat sink. The bottom surface of the MCHS is assumed to be taking the heat directly from the heat source and the all other surfaces are considered as insulated. In the present work, three MCHS models (model 2 to model 4) are investigated and the outcomes of these models are compared with the MCHS model (Model 1) without PCM. The studied models are,

Model 1 (M1): MCHS without PCM

Model 2 (M2): MCHS with PCM in single channel at the bottom

Model 3 (M3): MCHS with PCM in single channel at the top

Model 4 (M4): MCHS with PCM in divided channels at the bottom

Figure 2 depicts the micro-channel heat sinks (MCHS) models without PCM and with PCM at different positions, which are scrutinized in the present work. Filled channels in the heat sink models indicates the PCM (Figure 2).

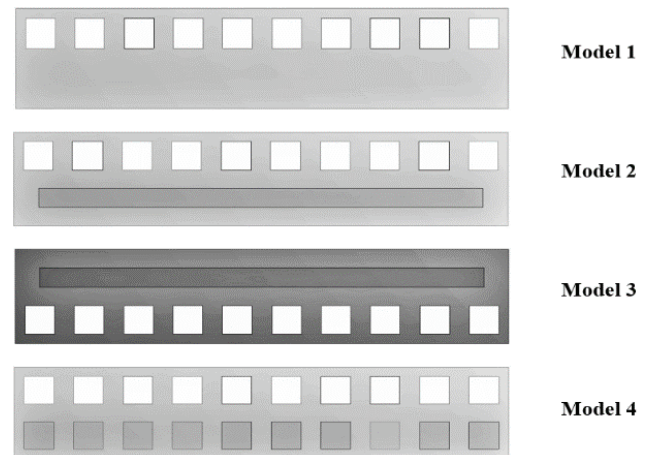


Figure 2. Front view images of all heat sink models.

MATHEMATICAL MODEL

Governing Equations

The equations which governs the Micro-channel flow are continuity, momentum equations, and energy equation. Those are, [31]

Continuity equation:

$$\frac{\partial u}{\partial x} + \frac{\partial v}{\partial y} + \frac{\partial w}{\partial z} = 0 \quad (1)$$

Momentum equations:

$$\rho \left(u \frac{\partial u}{\partial x} + v \frac{\partial u}{\partial y} + w \frac{\partial u}{\partial z} \right) = -\frac{\partial p}{\partial x} + \mu \left(\frac{\partial^2 u}{\partial x^2} + \frac{\partial^2 u}{\partial y^2} + \frac{\partial^2 u}{\partial z^2} \right) \quad (2)$$

$$\rho \left(u \frac{\partial v}{\partial x} + v \frac{\partial v}{\partial y} + w \frac{\partial v}{\partial z} \right) = -\frac{\partial p}{\partial x} + \mu \left(\frac{\partial^2 v}{\partial x^2} + \frac{\partial^2 v}{\partial y^2} + \frac{\partial^2 v}{\partial z^2} \right) \quad (3)$$

$$\rho \left(u \frac{\partial w}{\partial x} + v \frac{\partial w}{\partial y} + w \frac{\partial w}{\partial z} \right) = -\frac{\partial p}{\partial x} + \mu \left(\frac{\partial^2 w}{\partial x^2} + \frac{\partial^2 w}{\partial y^2} + \frac{\partial^2 w}{\partial z^2} \right) \quad (4)$$

Energy equation:

$$u \frac{\partial T}{\partial x} + v \frac{\partial T}{\partial y} + w \frac{\partial T}{\partial z} = \frac{1}{\alpha} \left(\frac{\partial^2 T}{\partial x^2} + \frac{\partial^2 T}{\partial y^2} + \frac{\partial^2 T}{\partial z^2} \right) \quad (5)$$

Boundary conditions

In this simulation analysis, it was considered that the heat source (electronic devices) is connected directly to the MCHS bottom surface and all other surfaces are assumed as insulated. The boundary conditions implemented for this work are

- No slip condition at the walls of the channels,
- A uniform and constant heat flux condition at the MCHS bottom wall.
- All walls of the heat sink except bottom wall are assumed as insulated, so the adiabatic condition applied for those walls.
- The coupled wall boundary condition is applied at solid and liquid interfaces in the heat sink.

Inlet conditions implemented to the working fluid (water) are represented as

$$u = v = 0, w = v_{in} \text{ and } T_f = T_{in}. \quad (6)$$

The inlet temperature of working fluid T_{in} is fixed as 300K and pressure outlet is fixed outlet boundary condition. The material of MCHS substrate and working fluid are considered as Copper and Water respectively.

Assumptions

For solving the present numerical problem the following assumptions are considered,

- Thermo-physical properties of substrate material, PCM and working fluid are constant and not effected by temperature.
- The flow of working fluid is steady, incompressible and laminar.
- Influence of gravitational force and all other forces are neglected.
- Micro-channel walls are assumed as straight and smooth.

Thermo Physical Properties of PCM

Thermo physical properties of phase change material (PCM) used in the present investigation are listed in Table 2 [32,33].

The performance of the MCHS is analysed by using thermal resistance as the key parameter. Thermal resistance

Table 2. PCM Thermo-physical properties

S.No	Property	Value
1	Density (kg/m ³)	870 @300 K 780 @340 K
2	Viscosity (Kg/m-sec)	0.0057933
3	Thermal conductivity (W/ m-K)	0.24 @300K 0.22 @340K
4	Specific heat C _p (j/kg-K)	2900
5	Melting heat (j/Kg)	190000
6	Liquidus temperature (K)	331.8
7	Solidus temperature (K)	331

of heat sink models with PCM is measured and compared with heat sink without PCM. The average thermal resistance (R_T) of the MCHS can be calculated as, [34]

$$R_T = \frac{T_b - T_{in}}{q A_b} \quad \text{K/W} \quad (7)$$

Where, \bar{T}_b = Base mean temperature (K).

q = Applied heat flux at MCHS base.

A_b = Base area of the MCHS.

The difference of maximum temperature to minimum temperature of the bottom wall of the MCHS is another parameter used to estimate the temperature uniformity of heat sinks and compare the heat sinks performance. The liquid fraction indicates the fraction of PCM converted to liquid phase from solid phase.

NUMERICAL MODEL

Numerical Method

The present investigation was conducted using the numerical software ANSYS-FLUENT. For velocity-pressure coupling, the SIMPLE algorithm was implemented. Second order upwind scheme was applied for the discretization of equations of energy and momentum. A convergence criteria of 1×10^{-5} was applied for the momentum and continuity equations and 1×10^{-6} was applied for energy equation. The method of the present study represented as a flow chart in the Figure 3.

Grid Independent Study

Grid independent test for a numerical problem was performed to find the solution, which is insensitive to the grid size. The average temperature of bottom wall of MCHS was measured with increasing the elements count. The change in mean temperature value after the mesh size of 5133838 elements (point 7) was negligible (Figure 4), so the solution at this mesh size is considered as grid independent solution.

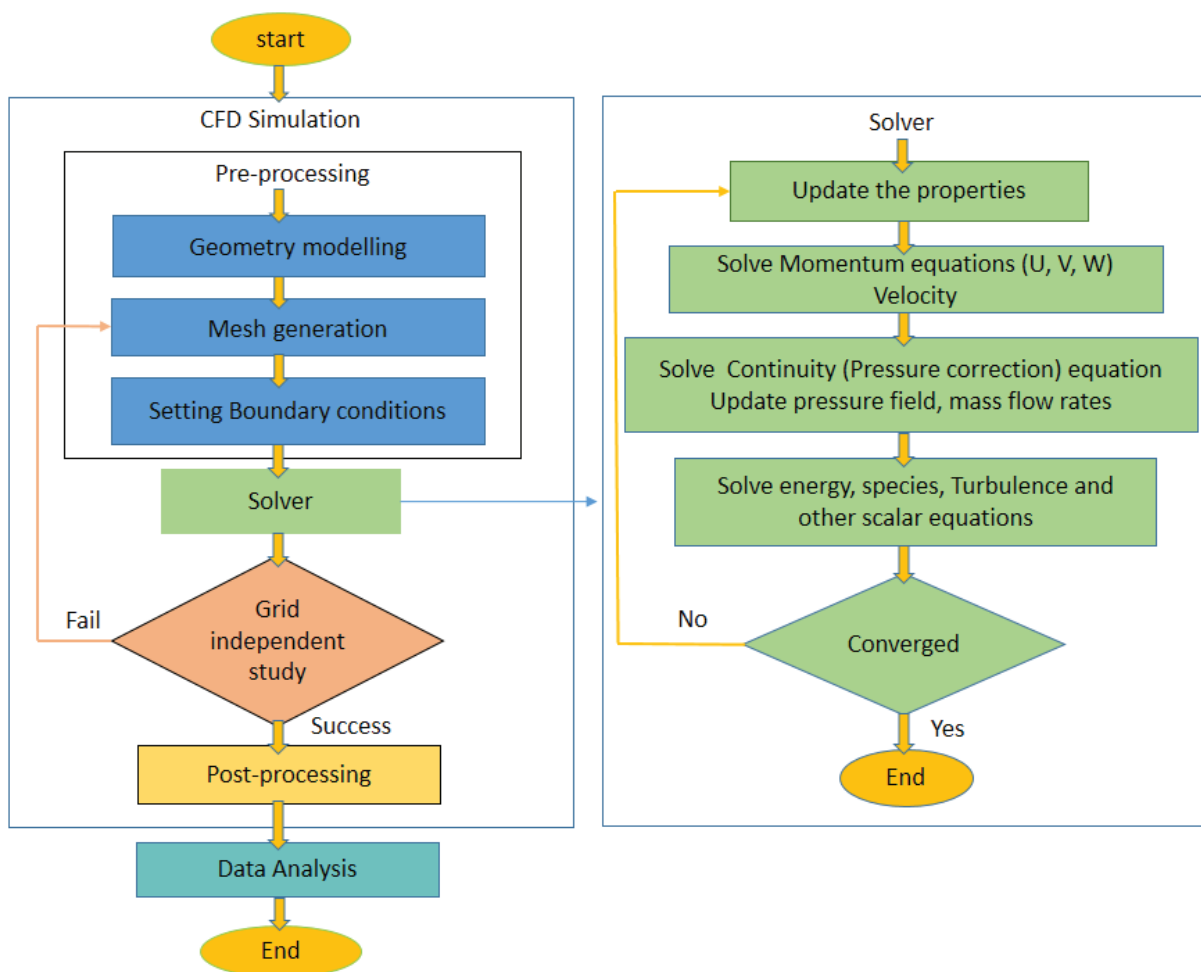


Figure 3. Numerical method followed in the present study.

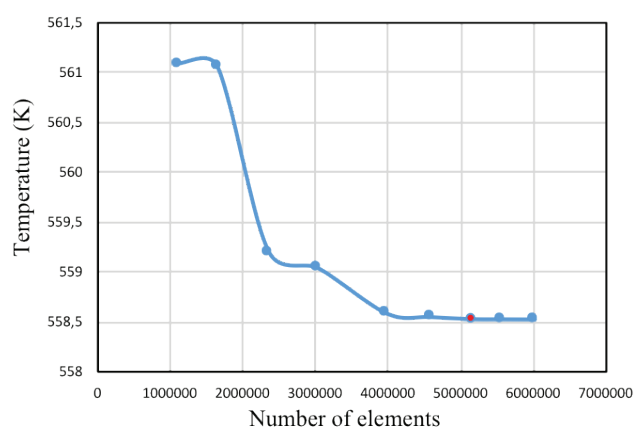


Figure 4. Average temperature variation at MCHS bottom wall with mesh size.

Validation of the model

The validation of present simulation model was done by comparing the results with existing experimental and numerical results of DB Tuckerman [4] and Wong KC and

Muezzin FNA[35] respectively. Good agreement of outcomes of the present model with literature was noticed with the maximum deviation of 2.35% and 3.81% with numerical & experimental results respectively. Results of validation work are presented in the Table 3.

RESULTS AND DISCUSSION

The findings of this numerical investigation are reported in this section. The outcomes were considered in the range of Reynolds number (Re) from 100 to 2000 and working fluid inlet temperature of 300K. Thermal resistance of all heat sink models was calculated and compared to analyse their performance. The variation of resistance in the range of heat flux from 10 to 160 W/cm² is presented in the Figure 5. The thermal resistance curves are straight lines in the Figure 5 because of the resistance is independent of the applied heat flux. From the figure 5, it is also observed that heat sink model 4 and model 3 have lower thermal resistance and model 2 has higher thermal resistance compared to the model 1 (MCHS without PCM). Lower thermal resistance

Table 3. Comparison of present numerical model with existing numerical & experimental models

Channel Width x height ($\mu\text{m} \times \mu\text{m}$)	Heat flux (W/cm^2)	Flow rate (cm^3/s)	Thermal resistance (R_f) (K/W)			Deviation (%)	
			Exp. results [4]	Num. results [35]	Present work	With Exp. results	With Num. results
56 x 320	181	4.7	0.110	0.108	0.1058	3.81	2.03
55 x 287	277	6.5	0.113	0.113	0.1103	2.35	2.35
50 x 302	790	8.6	0.090	0.093	0.0911	1.22	2.04

in heat sink model 3 and model 4 is observed because of the enhancement of heat transfer rate during phase changing process of PCM. 7.3% reduction in the thermal resistance of model 3 is noticed at the Re 200.

The reverse effect was noticed in case of heat sink model 2, because of the position of the PCM. When the PCM introduced in between heat source wall and fluid flowing channels (model 2), PCM acts as resistance for heat flow because of its lower thermal conductivity compared to the heat sink material. From this observation, it is clear that PCM improved the thermal performance of heat sink when it is placed above the working fluid flowing micro-channels. So, the position of PCM plays the key role in improving the performance of heat sink.

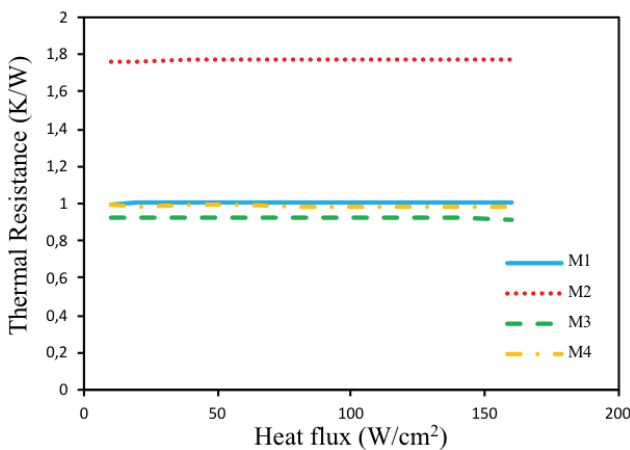


Figure 5. Thermal resistance (R_f) variation with applied heat flux.

Figure 6 shows the transient variation of liquid fraction. In Figure 6, liquid fraction of heat sink model 2, model 3 and model 4 is compared at two Reynolds numbers (Re) 200 and 400 for the time period of 30 seconds. For every model the liquid fraction values reaches maximum value (steady state) with in the 10 seconds only, because the quantity of PCM inserted in the MCHS is very less. Liquid fraction value decreased for all model when the Re increased

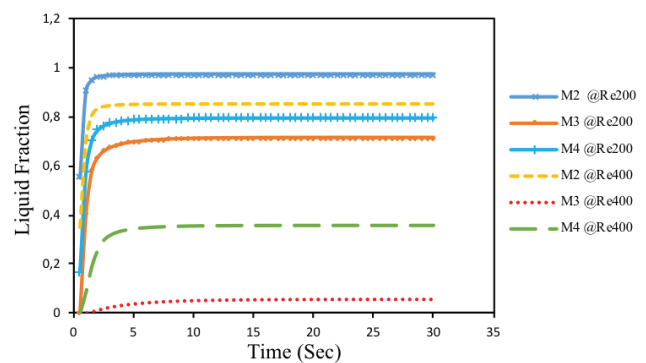


Figure 6. Transient variation of Liquid fraction of heat sink models.

from 200 to 400 because the amount of heat dissipated by the working fluid (water) is increased with Re, so the less amount of heat available for the PCM. Liquid fraction for the model 2 is higher in both cases because the PCM in the heat sink model 2 is nearer to the heat source and PCM absorbs the maximum heat by obstructing the heat dissipation to the working fluid.

Temperature is a direct parameter to scrutinize the heat sink characteristics. Figure 7 represents the variation of heat sink's bottom surface temperature along the length. It was pretended that the electronic component (heat source) is directly connected to the bottom surface of the MCHS, so the temperature of electronic component is same as the MCHS bottom surface temperature. Among the all models of MCHS, model 2 has higher temperatures even compared to MCHS without PCM because of high thermal resistance and heat sink model 3 has lower temperatures. It is also observed that the bottom surface temperature of MCHS rises along the length because of increase of working fluid temperature along the length when it is flowing inside the heat sink. From the above analysis, it is clear that model 3 shows the good performance with lowest heat sink temperatures among the four heat sink models.

An electronic component shows efficient performance at lower and uniform operating temperature conditions. This can be achieved by efficient thermal management

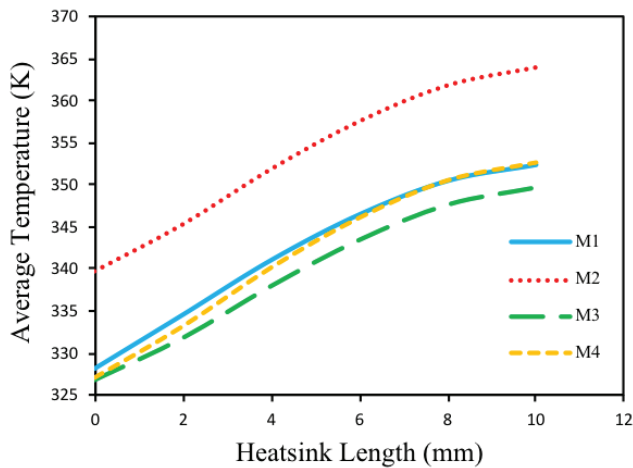


Figure 7. Variation of heat sink's bottom surface temperature along the length.

system with lower and uniform heat sink temperatures. The difference of maximum to minimum temperature of the heat sink represents its uniformity and Lower value of temperature difference indicates the more uniformity. Figure 8 represents the temperature uniformity of the four MCHS models. Among the four heat sink models, model 1(MCHS without PCM) has more temperature uniformity at lower Re (<400) and model 3 has more temperature uniformity at higher Re. The reason for the mentioned effect is, at lower Re PCM in the heat sink (model 2,3 and 4) is completely melted (liquid fraction 1) so at this phase PCM absorbed the sensible heat (much lower than latent heat).So heat sink without PCM has more temperature uniformity at lower Re.

At higher Re, PCM absorbed the more heat (latent heat) because PCM is in mixed phase, so more temperature uniformity witnessed in heat sinks with PCM.

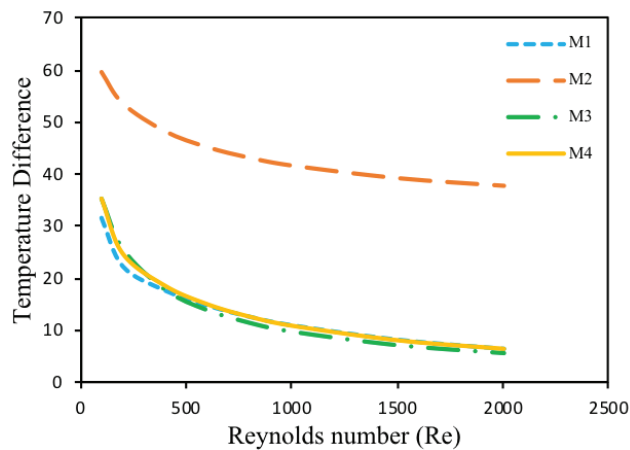


Figure 8. Variation of maximum to minimum temperature difference with Re.

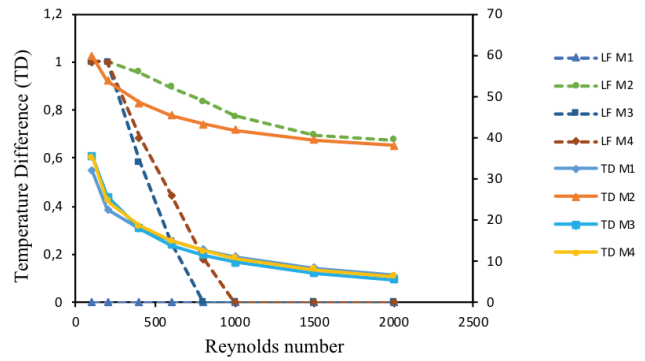


Figure 9. Variation temperature difference and Liquid Fraction with Reynolds number.

In case of heat sink model 3, 15.26% lower temperature difference was obtained at Re 2000 compared to the heat sink without PCM. This effect is clearly represented in the Figure 9, where the variation of liquid fraction (dotted lines) and temperature difference with Re is depicted. Figure 9 revealed that among the all MCHS models model 1 has the lowest temperature difference, when the liquid fraction value in the heat sink model 2, model 3 and model 4 is near 1 (PCM in liquid phase). So it can be concluded that PCM based heat sinks shows the improved performance during the phase changing process of PCM.

Figure 10 represents the 3-dimensional variation of liquid fraction with Re and heat flux for the heat sink model 3. From Figure 10, it is observed that the liquid fraction of heat sink was decreases with increasing the Re because of increase in heat taken away by the working fluid and it is obvious that the liquid fraction increases with the heat flux. As this graph (Figure 10) includes the combined effect of the heat flux and Re, it gives the information about the

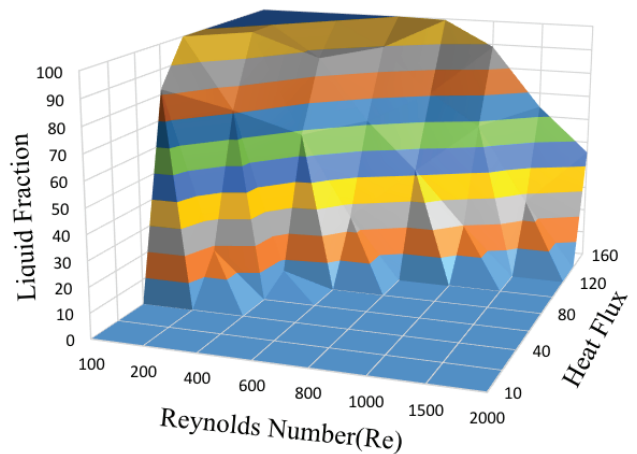


Figure 10. Variation of Liquid Fraction with Re and Heat flux for heat sink model 3.

required inlet conditions of the working fluid according to application. Figure 11 depicts the variation of Nu of the micro-channel flow with Re for the four heat sink models. From Figure 11, it is observed that the model 1 (MCHS without PCM) has the higher Nu among the four models because in model 1 the heat dissipation was done only by the working fluid but in remaining models PCM also absorbs the some of the heat. Even though the heat dissipated by the heat sink model 1 is less compared to the remaining three models, the heat dissipated by only working fluid is higher

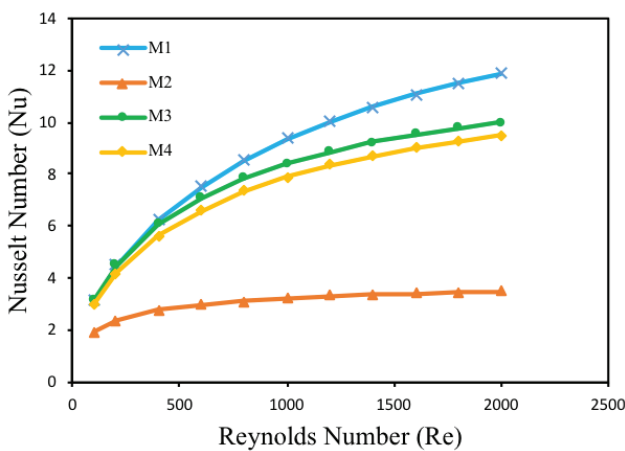


Figure 11. Variation of Nu with Re for four heat sink models.

in model 1 compared other models, this resulting the high Nu in model 1.

The temperature contours of MCHS cross-sections at various positions along the length for four models are presented in the Figure 12. These contours were extracted for four models at the Re of 200 and 100 W/cm² heat flux. It is clear from figure 8 that, the temperature is raised towards outlet from inlet and dropped towards the top of the MCHS. Highest values heat sink temperature values are noticed for model 2 because of high thermal resistance compared to other models.

Professional and social inferences

Thermal management is the primary consideration in the modern high capacity and compact electronic devices and processors. According to the Moore’s law, the transistors count in an integrated circuit (IC) is doubles for every two years. The modern requirement of high speed processors, ICs, fastest data transfer, high speed internet and compactness demands the efficient thermal management systems with large heat dissipating capacity. There is a thumb rule in literature that for 10°C increase in temperature, the life of the electronic components is reduced by half. The performance, reliability, speed and life of electronic devices are significantly improved by incorporating the suitable thermal management systems. The heat sink models proposed in this study are compact and very effective in heat dissipation. These heat sinks are appropriate for thermal management in the modern electronics and are expected to satisfy the demand for large heat dissipation.

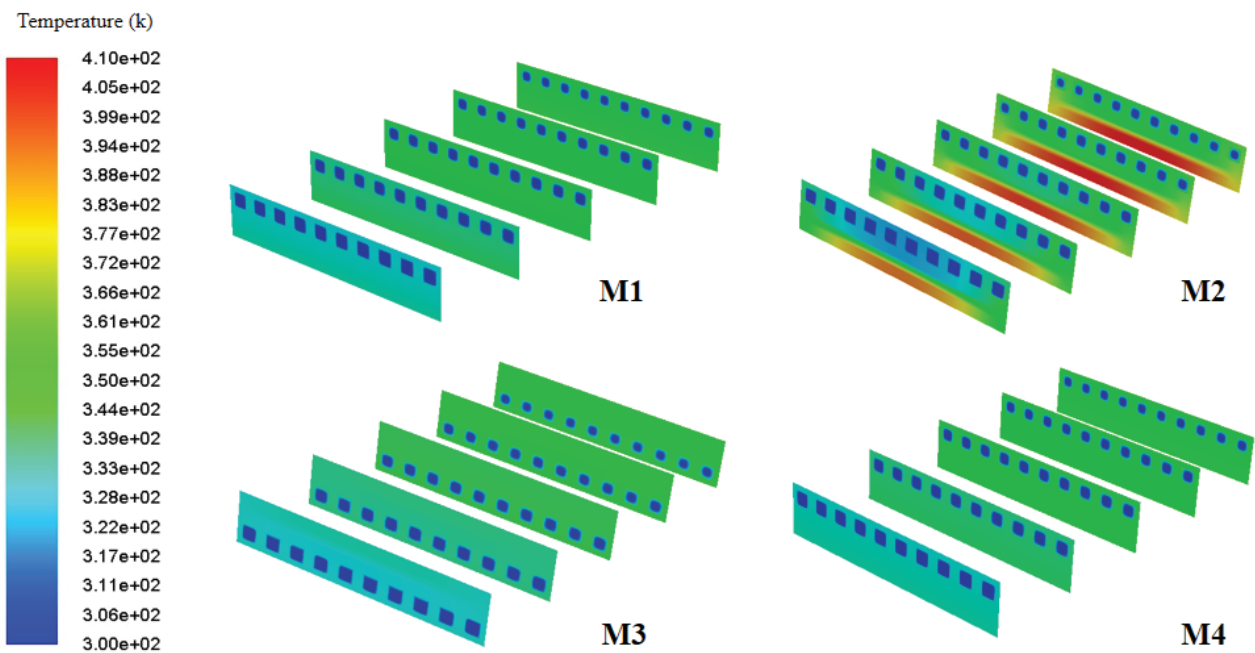


Figure 12 (M1 to M4). Temperature Contours for four models at Re 200 and heat flux of 100W/cm².

CONCLUSION

The present numerical investigation was conducted on MCHSs to augment their thermal performance by inserting the Phase change material (PCM). The computation model implemented for this analysis was compared with the existing literature and good agreement was found. Major conclusions drawn from this analysis are,

- The thermal performance of MCHS can be improved by introducing the PCM. A 7.3% decrement in thermal resistance was witnessed in the heat sink when the PCM was placed in a single channel at the bottom side (model 3) at a Reynolds number of 200.
- It was also observed that model 3 has 15.26% more temperature uniformity at Re 2000 compared to the MCHS without PCM.
- Among the four heat sink models compared, model 3 shows superior Performance with lower and uniform heat sink temperatures.
- It is also concluded that the PCM-based MCHSs show the better performance during the phase changing process of the PCM.
- Pressure drop was observed to be high in MCHS and the fabrication of these hybrid MCHSs is very expensive.

FUTURE SCOPE

In the present study, basic models of PCM based hybrid MCHS are developed and which are one of the better solutions for thermal management issues in electronic devices. There is more scope for improvement of efficiency and performance of these hybrid MCHS by optimizing the geometry of heat sink, using the suitable PCM and using the porous media to improve the heat transfer from PCM to substrate. The same method can be also implemented for mini channelled heat sinks used for other thermal management applications like battery cooling LED cooling etc.

NOMENCLATURE

A_b	Base area of the MCHS (m^2)
H	Heat sink height (m)
H_C	Micro-channel height (m)
H_p	PCM layer height (m)
L	Heat sink length (m)
p	Pressure (Pa)
q	Applied heat flux (W/m^2)
R_T	Thermal resistance ($K W^{-1}$)
t_1	MCHS top rib thickness (m)
t_2	MCHS bottom rib thickness (m)
T_b	Base average temperature (K)
T_f	Fluid temperature (K)
T_{in}	Fluid Inlet temperature (K)
v_{in}	Fluid inlet velocity (m/s)
W	MCHS Width (m)
W_c	Micro-channel Width (m)
W_p	PCM layer width(m)

W_t	Rib thickness between the channels (m)
x, y, z	Cartesian coordinates (m)

Abbreviations

MC	Micro-channel
MCHS	Micro-channel heat sink
MEPCM	Micro-encapsulated PCM
PCM	Phase change material
Nu	Nusselt number
Re	Reynolds number

Greek symbols

μ	Dynamic viscosity (Pa-s)
ρ	Density (Kg/m^3)
α	Thermal diffusivity (m^2/s)

Subscripts

b	Micro-channel Base
C	Micro-channel
f	Working Fluid
in	Inlet
T	Total

AUTHORSHIP CONTRIBUTIONS

Authors equally contributed to this work.

DATA AVAILABILITY STATEMENT

The authors confirm that the data that supports the findings of this study are available within the article. Raw data that support the finding of this study are available from the corresponding author, upon reasonable request.

CONFLICT OF INTEREST

The author declared no potential conflicts of interest with respect to the research, authorship, and/or publication of this article.

ETHICS

There are no ethical issues with the publication of this manuscript.

REFERENCES

- [1] Lan Y, Feng Z, Huang K, Zhang J, Hu Z. Effects of truncated and offset pin-fins on hydrothermal performance and entropy generation in a rectangular microchannel heat sink with variable fluid properties. *Int Commun Heat Mass Transf* 2021;124:105258. [\[CrossRef\]](#)
- [2] Ho CJ, Liu YC, Ghalambaz M, Yan WM. Forced convection heat transfer of Nano-Encapsulated Phase Change Material (NEPCM) suspension in a mini-channel heatsink. *Int J Heat Mass Transf* 2020;155:119858. [\[CrossRef\]](#)

- [3] Ma Y, Shahsavari A, Talebizadehsardari P. Two-phase mixture simulation of the effect of fin arrangement on first and second law performance of a bifurcation microchannels heatsink operated with biologically prepared water-Ag nanofluid. *Int Commun Heat Mass Transf* 2020;114:104554. [CrossRef]
- [4] Tuckerman DB, Pease RFW. High-performance heat sinking for VLSI. *IEEE Electron Device Lett* 1981;2:126–129. [CrossRef]
- [5] Mokrane M, Lounis M, Announ M, Ouali M, Djebiret MA, Bourouis M. Performance Analysis Of A Micro Heat Exchanger In Electronic Cooling Applications. *J Therm Eng* 2021;7:774–790. [CrossRef]
- [6] Gaikwad VP, Mohite SS. Performance analysis of microchannel heat sink with flow disrupting pins. *J Therm Eng* 2022;8:402–425. [CrossRef]
- [7] Rana S, Dura HB, Bhatrai S, Shrestha R. Impact of baffle on forced convection heat transfer of CuO/water nanofluid in a micro-scale backward facing step channel. *J Therm Eng* 2022;8:310–322. [CrossRef]
- [8] Kumar S, Sarkar M, Singh PK, Lee PS. Study of thermal and hydraulic performance of air cooled minichannel heatsink with novel geometries. *Int Commun Heat Mass Transf* 2019;103:31–42. [CrossRef]
- [9] Aryan Saini R, Vohra M, Singh A, Rabbani T, Choudhary M. Comparative thermal performance evaluation of a heat sink based on geometrical and material amendments: A numerical study. *Mater Today Proc* 2022;50:816–822. [CrossRef]
- [10] Bayer Ö, Baghaei Oskouei S, Aradag S. Investigation of double-layered wavy microchannel heatsinks utilizing porous ribs with artificial neural networks. *Int Commun Heat Mass Transf* 2022;134:105984. [CrossRef]
- [11] Kose HA, Yildizeli A, Cadirci S. Parametric study and optimization of microchannel heat sinks with various shapes. *Appl Therm Eng* 2022;211:118368. [CrossRef]
- [12] Gorzin M, Ranjbar AA, Hosseini MJ. Experimental and numerical investigation on thermal and hydraulic performance of novel serpentine minichannel heat sink for liquid CPU cooling. *Energy Rep* 2022;8:3375–3385. [CrossRef]
- [13] Qasem NAA, Zubair SM. Compact and microchannel heat exchangers: A comprehensive review of air-side friction factor and heat transfer correlations. *Energy Convers Manag* 2018;173:555–601. [CrossRef]
- [14] Sahar AM, Wissink J, Mahmoud MM, Karayiannis TG, Ashrul Ishak MS. Effect of hydraulic diameter and aspect ratio on single phase flow and heat transfer in a rectangular microchannel. *Appl Therm Eng* 2017;115:793–814. [CrossRef]
- [15] Ji Y, Yuan K, Chung JN. Numerical simulation of wall roughness on gaseous flow and heat transfer in a microchannel. *Int J Heat Mass Transf* 2006;49:1329–1339. [CrossRef]
- [16] Soleimanikutanaei S, Ghasemisahebi E, Lin CX. Numerical study of heat transfer enhancement using transverse microchannels in a heat sink. *Int J Therm Sci* 2018;125:89–100. [CrossRef]
- [17] Wang G, Qian N, Ding G. Heat transfer enhancement in microchannel heat sink with bidirectional rib. *Int J Heat Mass Transf* 2019;136:597–609. [CrossRef]
- [18] Zhang Y, Wang S, Ding P. Effects of channel shape on the cooling performance of hybrid micro-channel and slot-jet module. *Int J Heat Mass Transf* 2017;113:295–309. [CrossRef]
- [19] Kuppusamy NR, Mohammed HA, Lim CW. Numerical investigation of trapezoidal grooved microchannel heat sink using nanofluids. *Thermochim Acta* 2013;573:39–56. [CrossRef]
- [20] Kuppusamy NR, Mohammed HA, Lim CW. Thermal and hydraulic characteristics of nanofluid in a triangular grooved microchannel heat sink (TGMCHS). *Appl Math Comput* 2014;246:168–183. [CrossRef]
- [21] Ghale ZY, Haghshenasfard M, Esfahany MN. Investigation of nanofluids heat transfer in a ribbed microchannel heat sink using single-phase and multiphase CFD models. *Int Commun Heat Mass Transf* 2015;68:122–129. [CrossRef]
- [22] Manay E, Akyürek EF, Sahin B. Entropy generation of nanofluid flow in a microchannel heat sink. *Results Phys* 2018;9:615–624. [CrossRef]
- [23] Rostami J, Abbassi A. Conjugate heat transfer in a wavy microchannel using nanofluid by two-phase Eulerian-Lagrangian method. *Adv Powder Technol* 2016;27:9–18. [CrossRef]
- [24] Saeed M, Berrouk AS, AlShehhi MS, AlWahedi YF. Numerical investigation of the thermohydraulic characteristics of microchannel heat sinks using supercritical CO₂ as a coolant. *J Supercrit Fluids* 2021;176:105306. [CrossRef]
- [25] Mozafari M, Lee A, Mohammadpour J. Thermal management of single and multiple PCMs based heat sinks for electronics cooling. *Therm Sci Eng Prog* 2021;23:100919. [CrossRef]
- [26] Mahdi JM, Mohammed HI, Talebizadehsardari P. A new approach for employing multiple PCMs in the passive thermal management of photovoltaic modules. *Sol Energy* 2021;222:160–174. [CrossRef]
- [27] Alehosseini E, Jafari SM. Nanoencapsulation of phase change materials (PCMs) and their applications in various fields for energy storage and management. *Adv Colloid Interface Sci* 2020;283:102226. [CrossRef]
- [28] Deng X, Wang S, Wang J, Zhang T. Analytical modeling of microchannel heat sinks using microencapsulated phase change material slurry for chip Cooling. *Procedia Eng* 2017;205:2704–2711. [CrossRef]
- [29] Ho CJ, Chang PC, Yan WM, Amani P. Efficacy of divergent minichannels on cooling performance of heat sinks with water-based MEPCM suspensions. *Int J Therm Sci* 2018;130:333–346. [CrossRef]

-
- [30] Yan WM, Ho CJ, Tseng YT, Qin C, Rashidi S. Numerical study on convective heat transfer of nanofluid in a minichannel heat sink with micro-encapsulated PCM-cooled ceiling. *Int J Heat Mass Transf* 2020;153:119589. [\[CrossRef\]](#)
- [31] Rajabifar B. Enhancement of the performance of a double layered microchannel heatsink using PCM slurry and nanofluid coolants. *Int J Heat Mass Transf* 2015;88:627–635. [\[CrossRef\]](#)
- [32] Su W, Darkwa J, Kokogiannakis G. Review of solid-liquid phase change materials and their encapsulation technologies. *Renew Sustain Energy Rev* 2015;48:373–391. [\[CrossRef\]](#)
- [33] Yadav A, Soni S. Simulation of melting process of a phase change material (PCM) using ANSYS (Fluent). *Int Res J Eng Technol* 2017;2395–2356.
- [34] Al-Rashed AAAA, Shahsavari A, Rasooli O, Moghimi MA, Karimipour A, Tran MD. Numerical assessment into the hydrothermal and entropy generation characteristics of biological water-silver nano-fluid in a wavy walled microchannel heat sink. *Int Commun Heat Mass Transf* 2019;104:118–126. [\[CrossRef\]](#)
- [35] Wong KC, Muezzin FNA. Heat transfer of a parallel flow two-layered microchannel heat sink. *Int Commun Heat Mass Transf* 2013;49:136–140. [\[CrossRef\]](#)